ORIGINAL ARTICLE

Hematopoietic Stem Cells Mobilized by Granulocyte Colony-Stimulating Factor Partly Contribute to Liver Graft Regeneration After Partial Orthotopic Liver Transplantation

Feng Liu,[1] Xiaoben Pan,[1] Guodong Chen,[2] Dong Jiang,[1] Xu Cong,[1] Ran Fei,[1] and Lai Wei [1]
[1]*Hepatology Institute and* [2]*Department of Gastroenterology, Peking University People's Hospital, Beijing, China*

On the basis of the recently recognized potential of hematopoietic stem cells (HSCs) to give rise to hepatocytes, we investigated whether HSCs mobilized by granulocyte colony-stimulating factor (G-CSF) or G-CSF per se could contribute to faster recovery and promote tissue reparation after rats' (cross-sex) partial orthotopic liver transplantation (PLTx). Sex-mismatched (female to male) syngeneic rat PLTx was established. The recipients were repeatedly administrated recombinant G-CSF for 5 consecutive days before (G-CSF + PLTx group) and after PLTx (PLTx + G-CSF group). Compared with those in PLTx group, $CD34^+$ cells in peripheral blood and portal tract region increased from day 1 to 7 after transplantation in G-CSF + PLTx group and from day 3 to 14 after transplantation in PLTx + G-CSF group, respectively, which suggested that $CD34^+$ HSCs were mobilized and migrated into liver graft. Compared with that in G-CSF + PLTx and PLTx groups, there was a higher survival rate in the PLTx + G-CSF group. On day 3 after surgery, the level of aspartate aminotransferase and alanine aminotransferase were lower, whereas the mitosis index, proliferating cell nuclear antigen–positive nuclei, bromodeoxyuridine (BrdU) incorporation, and graft-to-recipient weight ratio were higher in the PLTx + G-CSF group. In contrast, these parameters had no significant difference between G-CSF + PLTx and PLTx groups. To define the origin of proliferating cells reconstituting liver after injury, sry^+ (sex-determining region for Y chromosome) and sry^+/cytokeratin 19^+ (CK19) cells were quantitated. Higher percentage of sry^+ and $sry^+/CK19^+$ cells in PLTx + G-CSF was detected than in G-CSF + PLTx groups on day 14 after surgery, although the liver engraftment rate still remained rather low. Some of the $sry^+/CK19^+$ cells in the portal tract areas were similar to hepatic oval cells/cholangiocytes. In conclusion, G-CSF administration after PLTx greatly improved survival rate and liver regeneration of partial graft, partly by its mobilizing HSCs into the injured liver to differentiate into hepatocytes through hepatic oval cells'/cholangiocytes' engraftment. ***Liver Transpl 12:1129-1137, 2006.***

Received July 10, 2005; accepted March 28, 2006.

Growing organ shortages for transplantation has led to an increase in partial orthotopic liver transplantation (PLTx). The major concern of PLTx is the adequacy of the size of the graft[1,2]: a small-for-size graft may not only be functionally inadequate for the recipient, but will also sustain injury characterized by rejection and ischemic injury, and result in inadequate regeneration, leading to hepatic insufficiency or liver failure. There-

Abbreviations: HSCs, hematopoietic stem cells; G-CSF, granulocyte colony-stimulating factor; PLTx, partial orthotopic liver transplantation; AST, aspartate aminotransferase; ALT, alanine aminotransferase; PCNA, proliferating cell nuclear antigen; BrdU, bromodeoxyuridine; GRWR, graft-to-recipient weight ratio; sry, sex-determining region for Y chromosome; CK19, cytokeratin 19; H&E, hematoxylin and eosin; PE, phycoerythrin; FITC, fluorescein isothiocyanate; SSC, standard saline citrate; DAPI, 4,6-diamidino-2-phenylindole.

Supported by the National High Technology Research and Development Program of China (863 Program) (2001AA216031) from Administration of Science and Technology of China, Chinese Basic Research Foundation (973) (2005CB522902), Ministry of Education of PR China (20040001133).

Address reprint requests to Lai Wei, MD, Professor, Hepatology Institute, Peking University People's Hospital, No.11 Xizhimen South Street, Beijing 100044, China. Telephone: 8610-68314422 ext. 5730; FAX: 8610-68322662; E-mail: weelai@163.com

DOI 10.1002/lt.20822
Published online in Wiley InterScience (www.interscience.wiley.com).

fore, improvement of liver regeneration capacity is important in partial liver transplantation, and therapy promoting limited small liver to regenerate remains to be developed.

Recent studies suggested that hematopoietic stem cells (HSCs) can differentiate into nonhematopoietic lineages in vivo, including skeletal[3] and cardiac myoblasts[4]; vascular endothelium[5]; epithelial cells of lung, gut, and skin[6]; and neuroectodermal cells.[7,8] Although it is not yet clear whether the underlying cellular mechanism of this apparent plasticity is transdifferentiation of HSCs[9-11] or cell fusion between HSCs and target cells,[12,13] there are several reports on the ability of HSCs to generate hepatocytes under tissue stress in mice and humans.[14-18] Therefore, it has been proposed that HSCs migration into sites of injury may be a mechanism by which damaged tissues are repaired.[19] However, the role of HSCs in the regeneration of damaged liver is unknown and is less understood for this process.

In current clinical practice, circulating HSCs numbers can be increased by mobilization from the bone marrow with granulocyte colony-stimulating factor (G-CSF).[20,21] And the mobilization of HSCs by G-CSF has been shown to be involved in the reparation of the infarcted heart.[22,23] Also, G-CSF is reported to be able to enhance hepatocyte regeneration.[24,25] Therefore, we decided to address whether G-CSF–mobilized HSCs or G-CSF per se could contribute to faster recovery and promote the regeneration process after rats' (cross-sex) PLTx.

MATERIALS AND METHODS

Animals

Inbred Sprague-Dawley rats (Academy of Military Medical Science, China), weighing 250-300 g each, were used. All the rats were housed in a standard animal laboratory with free activity and free access to water and chow. They were kept under constant environmental conditions with a 12-hour light-dark cycle. The rats were fasted 12 hours before operation. All the operations were performed under clean conditions. The studies met the National Research Council's guide for the care and use of laboratory animals.

Experimental Procedure

The experiment was conducted in 3 groups of rats. For the PLTx + G-CSF group, 3 hours after PLTx, recipients were mobilized by subcutaneous injections daily with 50 μg/kg per injection recombinant human G-CSF (Filgrastim Neupogen, Kirin, Tokyo, Japan) for 5 consecutive days from day 0 to day 4. For the G-CSF + PLTx group, before PLTx, recipients were mobilized by subcutaneous injections daily with 50 μg/kg per injection G-CSF for 5 consecutive days from day 0 to day 4. On the fifth day, PLTx was conducted. In the PLTx group, recipients were injected with the same volume of saline. Six animals were killed at each time point at days 1, 3, 5, 7, and 14 after transplantation. One hour before they were killed, rats were given bromodeoxyuridine (BrdU; Sigma-Aldrich, St. Louis, MO, USA), dissolved in water, intraperitoneally at a dose of 100 mg/kg body weight. At the time they were killed, graft-to-recipient weight ratio (GRWR) was calculated. Portions of the liver and duodenum were fixed in 10% formalin for 18-24 hours, then processed and embedded in paraffin for histological evaluation. The remains of the liver was frozen in liquid nitrogen and stored at −80°C. Blood was obtained from the inferior vena cava for estimation of serum alanine aminotransferase (ALT) and aspartate aminotransferase (AST) activities when animals were killed.

Liver Transplantation

For transplantation, donors (female Sprague-Dawley rats) and recipients (male Sprague-Dawley rats) were anesthetized with ether. Liver reduction was achieved by removing left lateral, left median, and anterior and posterior caudate lobes, which resulted in a 50% reduction in the liver mass, as described by Omura et al.[26] The graft was flushed and stored in cold saline with a target cold ischemic time of 60 minutes. The PLTx was performed according to the cuff technique of Kamada and Calne,[27] without hepatic artery reconstruction. The suprahepatic vena cava was reconstructed with continuous 8-0 polypropylene sutures. The portal vein was reanastomosed by using the cuff technique modified from the method of Kamada and Calne. When the anastomosis of portal vein and suprahepatic vena cava was completed, the liver was reperfused. The anastomosis of infrahepatic vena cava was then completed by the same cuff technique. The bile duct was anastomosed with an intraluminal stent. The transplantation procedure required less than 60 minutes, during which time the portal vein was clamped for 17 to 22 minutes.

Survival Study

Ten rats in each group were used for the survival study. Rat deaths within 48 hours of operation were considered as technical failures and their data excluded from further analysis.

Evaluation of Histology and Regeneration

For histological analysis of liver grafts, paraffin-embedded 6-μm-thick sections were stained with hematoxylin and eosin (H&E) and based on a semiquantitative scoring system for nonspecific liver damage as previously described.[28] For evaluating regeneration, mitotic activity in the livers was observed in 6-μm-thick sections stained with H&E. Paraffin sections were stained with antibodies of proliferating cell nuclear antigen (PCNA) and BrdU (Santa Cruz Biotechnology, Santa Cruz, CA, USA). The immunohistochemistry was performed with a commercial kit (Zymed LAB-SA System; Zymed Laboratories, South San Francisco, CA, USA). The hepatic labeling index was calculated as the number of PCNA- and BrdU-labeled nuclei for 1,000 hepatocyte nuclei.

Duodenal tissue sections served as a positive control for adequate uptake of BrdU and labeling. In addition, mitotic activity was also evaluated by counting 1,000 hepatocytes in each liver.

HSCs Mobilization

Flow cytometry analysis was done on a FACSCalibur flow cytometer (Becton Dickinson, San Jose, CA, USA). The $CD34^+$ cells (phycoerythrin [PE]-conjugated rabbit anti-rat CD34; Becton Dickinson) were analyzed in a gate defined by CD45 antigen expression (fluorescein isothiocyanate [FITC]-conjugated mouse anti-rat CD45; Harlan Lab, England). Mouse isotype controls (FITC-IgG1, PE-IgG1; Becton Dickinson) were used to account for unspecific fluorescence.

The mononuclear cells were isolated by Ficoll-Paque (Amersham Pharmacia Biotech, Freiburg, Germany) density gradient centrifugation of heparinized ethylenediaminetetraacetic acid (EDTA) blood samples obtained from normal control animals and the recipient rats. The cells were suspended in FACS buffer (phosphate-buffered saline [PBS] supplemented with 5% fetal bovine serum and containing 0.05% NaN_3) at a concentration of about 1,000,000 cells/mL. The cells were washed by centrifugation in 3 volumes of FACS buffer and resuspended in 50 μL FACS buffer containing primary antibody for 40 minutes at 4°C. Cells were washed 3 times with FACS buffer and fixed in PBS/4% paraformaldehyde for 30 minutes on ice for analysis.

Immunohistochemistry of CD34 Antigen

Immunohistochemical detection was performed on frozen sections after 10 minutes' fixation in cold acetone. The 6-μm-thick sections were incubated in a 1:10 dilution of anti-rat polyclonal CD34 antibody (Santa Cruz Biotechnology). The immunohistochemistry was performed with a commercial kit (Zymed LAB-SA System; Zymed Laboratories). Peroxidase activity was determined by diaminobenzidine staining. The sections were counterstained with hematoxylin. Positive cells were counted at 400× magnification. Ten random fields were observed in each of the liver portal tract areas. The sum of the positive cells from 10 fields was multiplied by a factor of 1.6 to yield the cell count/mm^2 tissue.

In Situ Hybridization of Y Chromosomes

The probe was derived from the sequence of sex-determining region for Y chromosome (sry) and was a 104-bp polymerase chain reaction product amplified from male genomic DNA by using PCR DIG Probe Synthesis Kit (Boehringer Mannheim, Germany). The primer sequences were F, CAT CGA AGG GTT AAA GTG CCA and R, ATA GTG TGT AGG TTG TTG TCC. The polymerase chain reaction was carried out under the following conditions in a thermal cycler (Perkin-Elmer/Cetus). After denaturation at 94°C for 5 minutes, 35 cycles of amplification were performed; each step consisted of denaturation at 94°C for 30 seconds, primer annealing at 56°C for 30 seconds, and chain elongation at 72°C for 45 seconds, followed by a final elongation step at 72°C for 7 minutes. The probe was purified with QIAquick Gel Purification Kit (Qiagen, Germany) according to the manufacturer's instructions.

The in situ hybridization reaction was performed on paraffin-embedded 6-μm tissue sections. After removal of paraffin, sections were treated by proteolytic digestion for 30 minutes at 37°C with 10 μg/mL proteinase K (Sigma-Aldrich) dissolved in 50 mM EDTA and 0.1 M Tris-HCl, followed by 2 rinses of 5 minutes each in 0.01 M PBS. After washing, the specimens were prehybridized for 30 minutes with buffer containing 10% dextran sulfate, 5× standard saline citrate (SSC), 5× Denhardt's solution (Roche Molecular Biochemicals, Germany), 100μg/mL salmon sperm DNA, and 50% deionized formamide (Sigma-Aldrich). Residual prehybridization buffer was removed from the tissue sections, and the appropriate digoxigenin probes, diluted in prehybridization buffer, were applied to sections. The sections were covered with silicone-coated coverslips (Sigma-Aldrich), denatured at 95°C for 5 minutes on a heat plate, and hybridized in humidified atmosphere at 37°C overnight. Upon completion of the hybridization reaction, the coverslips were removed and specimens were washed 3 times for 10 minutes each in 50% formamide in 2× SSC solution at 42°C, followed by 2 washes in 2× SSC for 5 minutes each. Five percent bovine serum albumin blocking reagent was then applied for 30 minutes, and drained away, then AP-conjugated sheep anti-digoxigenin antibody (Roche Molecular Biochemicals, Germany), diluted 1:10 in 5% bovine serum albumin was applied for 1 hour at 37°C. Sections were rinsed 3 times for 5 minutes each in 4× SSC/0.01% Tween solution at 42°C, and then reacted with nitroblue tetrazolium/5-bromocresyl-3-indolylphosphate chromogen (Roche Molecular Biochemicals, Germany) for 30 minutes. Sections were rinsed again and counterstained with 0.1% nuclear fast red and analyzed under a light microscope. Some tissue sections were processed without probe to serve as negative controls. sry^+ cells were evaluated by counting positive cells per 1,000 nuclei in each liver.

Double Immunostaining for sry and CK19

Liver tissues were sectioned vertically at 6-μm thickness. Fluorescence immunohistochemical double labeling was carried out by the indirect immunofluorescence method. The primary antibodies used in the experiments were goat anti-rat sry polyclonal antibody (1:40 dilution; Santa Cruz Biotechnology) and mouse anti-rat cytokeratin 19 (CK19) monoclonal antibody (1:100 dilution; Progen Biotechnik, Heidelberg, Germany). For double-labeling experiments, the sections were incubated in a mixture of 2 primary antibodies overnight at 4°C. After washing with PBS, binding sites of the primary antibodies were revealed by incubation in a mixture of 2 fluorochrome conjugates for 30 minutes at 37°C in the same medium as that used in incubating the primary antibodies: FITC-labeled rabbit anti-mouse

IgG (for CK19, 1:200 dilution; Dako, Denmark) plus PE-labeled rabbit anti-goat IgG (for sry, 1:100 dilution; Santa Cruz Biotechnology). After washing in PBS, the sections were coverslipped with a mounting medium containing DAPI (4,6-diamidino-2-phenylindole) counterstain (Vectashield; Vector Laboratories Inc., Burlingame, CA, USA), and examined with a Zeiss confocal fluorescence microscope equipped with a triple-band pass filter. Different controls were obtained by omitting one or both of the 2 primary antibodies during the incubation. Omission of one of the primary antibodies yielded only the immunoreactivity for the remaining antibody, while omission of both abolished any immunolabeling. Staining by a mixture of 2 secondary antibodies after incubation with 1 of the 2 primary antibodies showed no cross-reactivity of species-specific secondary antibodies. The proportion of $sry^+/CK19^+$ cells in each section was counted by digital photographs that had been taken from contiguous fields at 400× magnifications from sections. Fields were selected randomly and focused under a DAPI filter, then captured with that filter. Images were then sequentially captured with the FITC (CK19) filter and PE (sry) filter without changing focus, thus ensuring the same plane of analysis. All 3 filtered images were then digitally combined (DAPI, FITC for CK19, PE for sry) with cell counts derived from these combined images.

Statistical Analysis

Continuous variables were expressed as mean ± SD. Differences of continuous parameters among groups were analyzed; 1-way analysis of variance followed by Scheffé's post hoc test were used. A value of $P < 0.05$ was considered significant. Animal survival was evaluated by Kaplan-Meier plot. Significance was defined as $P < 0.05$. The data were analyzed by SPSS software version 11.0 (SPSS Inc., Chicago, IL, USA).

RESULTS

G-CSF Mobilization After PLTx Improved Rat Survival

Rat survivals were shown in Figure 1. In PLTx and G-CSF + PLTx group, the rate of survival at 7 days was similar (PLTx, 50%; 5 of 10; G-CSF + PLTx, 60%; 6 of 10). In contrast, in PLTx + G-CSF group, the rate of survival at 7 days was increased (90%; 9 of 10).

G-CSF Mobilization After PLTx Improved Liver Function

To determine the extent of liver injury in different G-CSF–mobilized PLTx, serum AST and ALT levels were measured. In 3 groups, AST and ALT levels of the recipient rats were initially elevated and decreased with time. In the PLTx + G-CSF group, AST and ALT activities presented significantly lower values from day 3 to 7 after operation when compared with the values found in PLTx and G-CSF + PLTx group at the same time points (Fig. 2A, B).

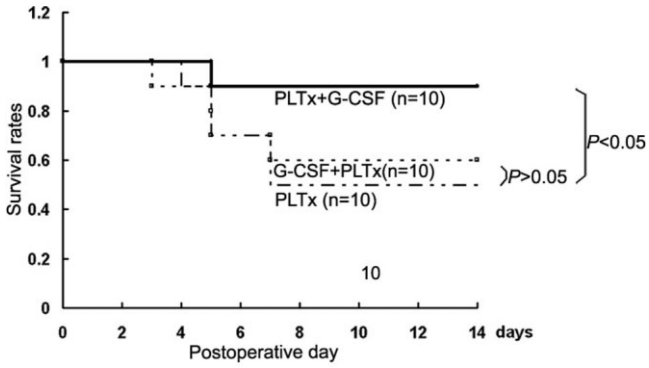

Figure 1. Survival curve after PLTx. Survival of rats was not significantly different between PLTx and G-CSF + PLTx. However, survival of rats in PLTx + G-CSF was significantly higher compared with that of PLTx and G-CSF + PLTx.

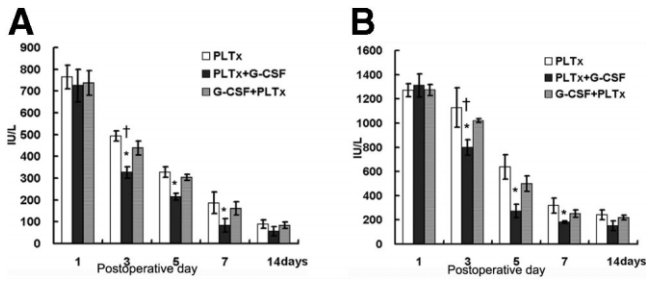

Figure 2. Serum ALT and AST activity after PLTx. (A) ALT and (B) AST activities after PLTx (mean ± SD) (n = 6). Vertical bars represent SD from mean. Statistical significance. †$P < .05$ for PLTx + G-CSF liver vs. G-CSF + PLTx and PLTx at different time points.*$P < .05$ for PLTx + G-CSF liver vs. G-CSF + PLTx and PLTx at same time points.

G-CSF Mobilization After PLTx Accelerated Restoration of Liver Graft

Histological findings in liver grafts were different in each group. Liver sections from rats of PLTx + G-CSF group rats, which received G-CSF after PLTx and were killed 5 days later, presented only scatter hepatocytic necrosis, maintaining a rather normal architecture. In contrast, livers from PLTx group and G-CSF + PLTx group rats, which received G-CSF only before PLTx, showed moderate necrosis around the portal tract areas and venous endothelial inflammation was mild to moderate. At 14 days after surgery, no hepatocytic necrosis was observed in the PLTx + G-CSF group, whereas in the PLTx group and the G-CSF + PLTx group, there was some degree of hepatocellular necrosis around the portal tract area and central vein (Fig. 3A-C); this was also confirmed by the damage score, which in the PLTx + G-CSF group was significantly lower than in the G-CSF + PLTx group and in PLTx ($P < 0.05$) (Fig. 3D). These findings suggest that the recovery process could be accelerated by mobilization with G-CSF after PLTx.

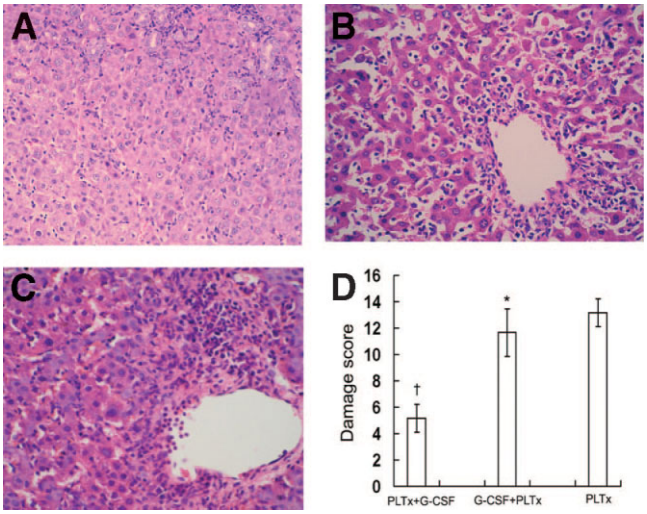

Figure 3. Histology of grafts on day 14 after PLTx. (A) H&E-stained liver section from PLTx + G-CSF group graft. Note normal histology of liver lobule. (B) Liver sections from PLTx group graft with focal and confluent hepatocytic necrosis in vicinity of central vein. (C) Liver sections from G-CSF + PLTx group graft with focal area of hepatocytic necrosis in vicinity of central vein (original magnification, 400×). (D) Comparison of total damage score on day 14 after PLTx. †$P < .05$ for PLTx + G-CSF liver vs. PLTx and G-CSF + PLTx.*$P > .05$ for G-CSF + PLTx vs. PLTx.

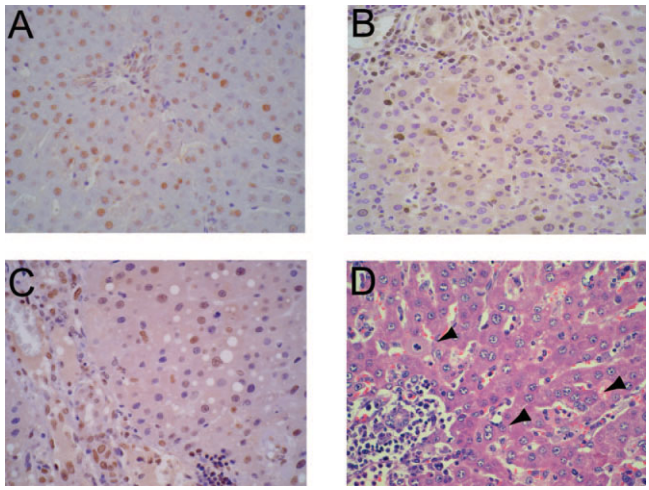

Figure 4. Hepatocyte-proliferative activity of liver grafts on 3 days after transplantation. Immunohistochemical staining of PCNA-positive hepatocytes. (A) PLTx + G-CSF group showed higher positive cell numbers than (B) G-CSF + PLTx group and (C) PLTx group. Brown-stained hepatocytes represent positive staining, indicating hepatocytes in S through M phases of cell cycle. H&E-stained section from (D) PLTx + G-CSF group reveals a great extent of hepatocyte mitosis (arrows). Original magnification, 200 × (A-C) and 400 × (D).

G-CSF Mobilization After PLTx Accelerated Liver Regeneration

Hepatocytes were mitotically quiescent in intact adult liver, as reflected by PCNA and BrdU labeling index of less than 1% (0.44 ± 0.25%) in control rats. The cells proliferating on day 3 after PLTx were predominantly in the periportal and midzonal regions of the liver (Fig. 4A-D). The results of mitotic activity, PCNA, BrdU incorporation, and GRWR studies that indicate regeneration are illustrated in Figure 5. The labeling and mitotic indices remained higher on day 3 in the PLTx + G-CSF group compared with those in the PLTx and G-CSF + PLTx groups. The maximum PCNA index of hepatocytes was 65.83 ± 13.00% for PLTx + G-CSF rats, 47.00 ± 6.81% for PLTx rats, and 52.00 ± 6.32% for G-CSF + PLTx rats, respectively ($P < 0.05$). BrdU labeling in hepatocytes also showed a similar pattern as that of PCNA-positive hepatocytes: lower than PCNA. From days 3 to 7 after surgery, GVWR in PLTx + G-CSF was significantly higher than in PLTx and G-CSF + PLTx ($P < 0.05$). The data suggest that regeneration of partial liver graft was promoted by G-CSF after PLTx.

G-CSF Stimulated HSCs Mobilization, Homing to Liver Graft After PLTx, and Differentiating Into Hepatocytes Through Hepatic Oval Cells/Cholangiocyte Engraftment

The change of $CD34^+$ cells in peripheral blood was shown in Figure 6A. After PLTx, the peripheral $CD34^+$cells in PLTx were increased on day 1, and then decreased. After G-CSF administration, the peripheral $CD34^+$ cells were significantly increased in PLTx. The $CD34^+$ cells in G-CSF + PLTx showed a greater increase on day 1, and decreased gradually thereafter. The $CD34^+$ cells in PLTx + G-CSF showed a greater increase than those in PLTx on day 3, were elevated until day 5, and decreased on the following days. Compared with PLTx group, $CD34^+$ cells in peripheral blood were increased from day 1 to 7 after transplantation in G-CSF + PLTx group and from day 3 to 14 after transplantation in PLTx + G-CSF group, respectively. Thus, there was a prolonged augmenting response of peripheral $CD34^+$ cells to G-CSF.

The change of $CD34^+$ cells in liver graft also showed a similar pattern as that in peripheral blood (Fig. 6B). In the PLTx + G-CSF group, $CD34^+$ cells mainly existed in portal tract area and necrosis area from days 3 to 7, whereas more $CD34^+$ cells were scattered in liver lobule on day 1 in the G-CSF + PLTx group (Fig. 7A-B).

In the male rats (positive control), sry^+ signals were observed in the majority of hepatocytes (Fig. 8A). In all male recipients of female liver graft, sry^+ cells could be detected periportally around the central vein, whereas some were arranged in the liver lobule. The G-CSF–mobilized group in particular demonstrated clusters of sry^+ cells arranged periportally (Fig. 8C, D). In contrast to the PLTx group, few sry^+ hepatocytes could be observed (Fig. 8E). Contaminated hematopoietic cells, preferentially arranged periportally, could also be easily distinguished by morphology and were excluded from counting. Enumeration of sry^+ cells in the liver parenchyma on day 14 after operation yielded a higher percentage of donor-origin hepatocytes in the G-CSF–mobilized group compared with that in PLTx group, and more sry^+ cells existed in the PLTx + G-CSF group than

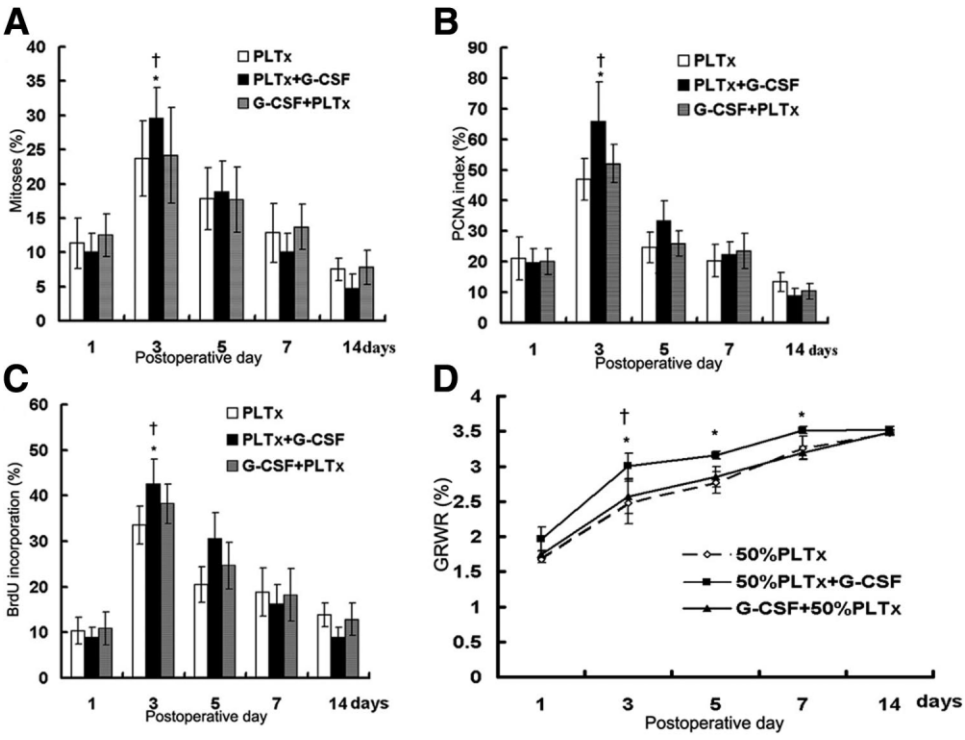

Figure 5. Hepatocyte-proliferative activity of liver grafts after transplantation. Percentage of (A) mitoses, (B) PCNA index, (C) BrdU incorporation, and (D) GRWR shown in 3 groups (mean ± SD). †P < .05 for PLTx + G-CSF liver vs. G-CSF + PLTx and PLTx at different time points. *P < .05 for PLTx + G-CSF liver vs. G-CSF + PLTx and PLTx at same time points.

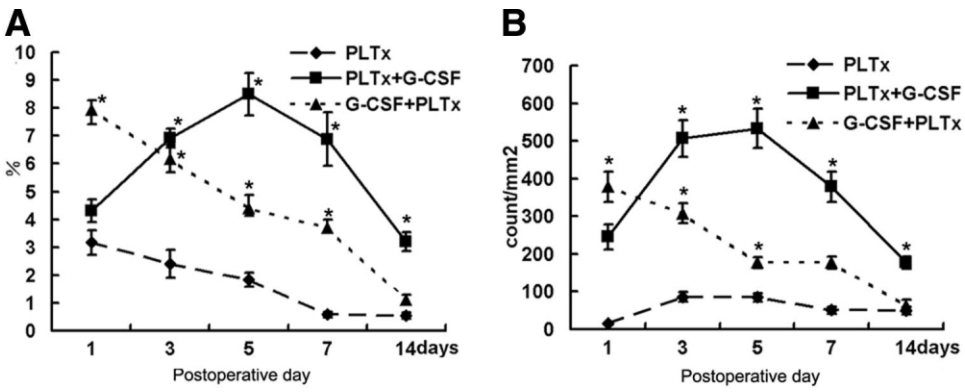

Figure 6. Change of $CD34^+$ cells in 3 groups. Change of $CD34^+$ cells (A) in peripheral blood were analyzed by FACS and (B) in liver grafts. *P < .05 for PLTx + G-CSF liver and G-CSF + PLTx vs. PLTx at same time points, respectively.

that in the G-CSF + PLTx group (1.68% vs. 0.77%) (Fig. 8F). Percentage of HSCs-derived hepatocytes in livers from the G-CSF–mobilized group of rats represented a rather low frequency of cells potentially capable of accelerating recovery and markedly improving survival of partial liver graft.

On day 14 after surgery, double staining for sry and CK19 demonstrated that some hepatic oval cells/cholangicytes in portal tract areas were $sry^+/CK19^+$ (Fig. 9A-G). There were more $sry^+/CK19^+$ cells in the portal tract region in the G-CSF–mobilized group than in the PLTx group, and more $sry^+/CK19^+$ cells in the PLTx + G-CSF group (33.8/400× magnification) than in the G-CSF + PLTx group (33.8/400× magnification) (Fig. 9I). Exposure to G-CSF increased the fraction of regenerating HSCs.

These data suggest that liver repair after injury might be partly mediated by HSCs mobilization.

DISCUSSION

The current study indicates that G-CSF administration after PLTx accelerates recovery from PLTx-induced liver injury. G-CSF exerts a beneficial effect on the regenerative process occurring in the liver graft, partly mediated by mobilizing HSCs that home to the injured liver and possibly differentiate into hepatocytes through hepatic oval cells/cholangiocytes.

It is well known that HSCs can be mobilized from bone marrow into circulating blood by G-CSF.[20,21,29] And G-CSF has been shown to be involved in the reparation of the infarcted heart.[22,23] Although Theocharis et al.[24,25] reported that single dose of G-CSF could accelerate and enhance hepatocyte proliferation in partially hepatectomized and fulminant hepatic failure (FHF)-induced rats as detected through serum biochemical and liver regeneration parameters, they did

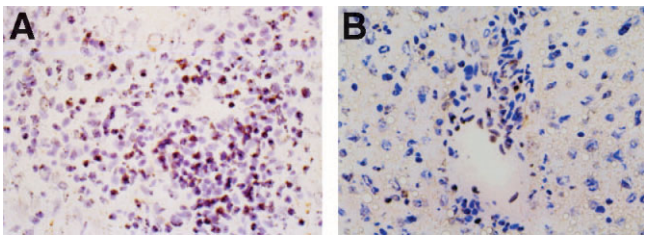

Figure 7. Immunohistochemical staining of CD34$^+$ cells. Brown-stained CD34$^+$ cells were mainly in portal tract areas. More CD34$^+$ cells were found on day 3 in (A) PLTx + G-CSF than in (B) PLTx. Original magnification, 400×.

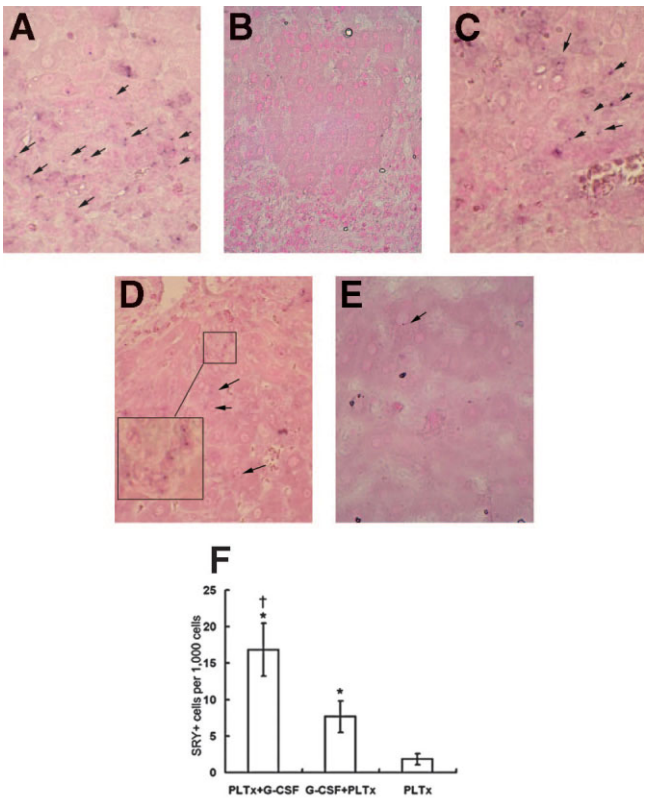

Figure 8. In situ hybridization for sry$^+$ cells (blue-purple dot, arrow) in liver. (A) Male liver specimen showing Y-chromosome signals (arrows) in hepatocytes. (B) Female liver specimen showing no Y-chromosome signals in hepatocytes. (C) Female-male isograft specimen in PLTx + G-CSF group and (D) in G-CSF + PLTx group showing Y-chromosome signals (arrows) in a few hepatocytes and bile duct epithelial cells. (E) Female-male isograft specimen in PLTx group showing few Y-chromosome signals (arrows) in hepatocytes. (F) Percentage of donor-origin and host-origin cells in liver graft on day 14 after transplantation. Number of sry$^+$ cells in G-CSF–mobilized group was more than that in PLTx (*P < .05). Number of sry$^+$ cells in PLTx + G-CSF group was more than that in G-CSF + PLTx group (†P < .05). Original magnification, 400× (A, C-E) and 300× (B).

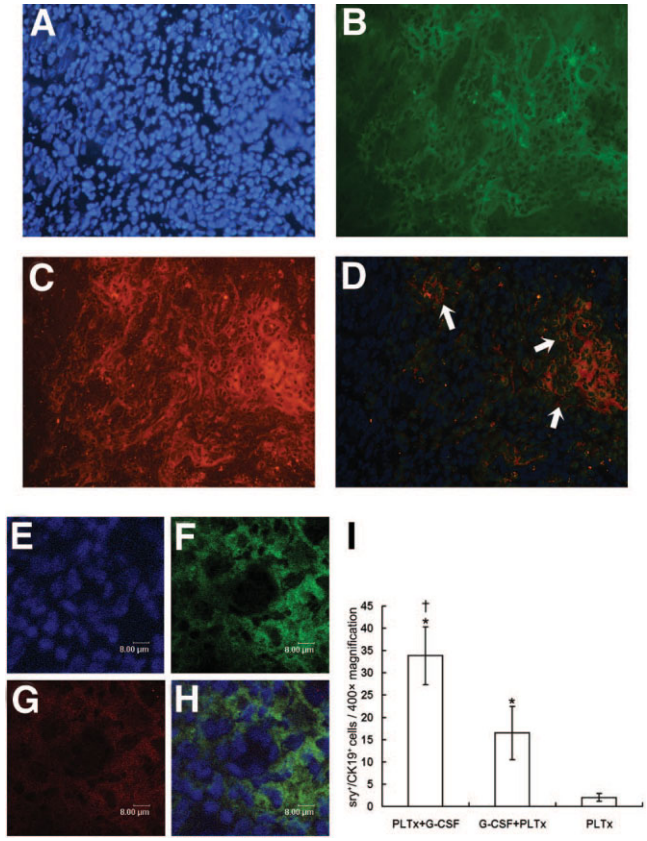

Figure 9. Double fluorescent immunohistochemistry for sry/CK19 in portal tract areas in PLTx + G-CSF on day 14 after surgery. (A, E) Nuclei were counterstained with DAPI staining (blue). (B, F) Green fluorescence shows CK19$^+$cells. (C, G) Red fluorescence shows sry$^+$ cells. (D) Merged figure of A, B, and C. (H) Merged figure of E, F, and G. (A-D) Image of reactive ductules and biliary-like cells (arrows) in portal tract areas (original magnification, 400×). (E-H) Image of biliary-like cells from confocal microscopy. (I) sry$^+$/CK19$^+$ cells per 400× magnification. Number of sry$^+$ cells in G-CSF–mobilized group was more than that in PLTx (*P < .05). Number of sry$^+$/CK19$^+$ cells in PLTx + G-CSF group was more than that in G-CSF + PLTx group (†P < .05).

not delineate the possible role of stem cells mobilized in liver regeneration. Combining these researches, it is proposed that G-CSF–mobilized HSCs may be involved in the repair of liver injury. To test whether HSCs mobilized by G-CSF has the capacity of raising hepatocytes, whether or G-CSF per se promotes hepatocyte regeneration in partial liver graft, we adopted the sex-mismatched rat PLTx model because the Y chromosome can be used as a specific marker of HSCs-derived hepatocytes.

HSCs' contribution to liver regeneration was evaluated by in situ hybridization for sry after sex-mismatched transplantation. More sry$^+$ and sry$^+$/CK19$^+$ cells were seen in the G-CSF–mobilized group than that in PLTx group, and more sry$^+$ and sry/CK19-positive cells in the PLTx + G-CSF group than in the G-CSF + PLTx group. But the level of liver chimerism was the same as the usually reported frequency of donor-derived hepatocytes (usually <0.2%) in injured animals.[14,30,31] Notably, only groups that had used the fumarylaetoacetate hydrolase mouse model, which offered a selective proliferative advantage in the transplanted cells, had displayed 30% to 50% liver regeneration with bone marrow–originated cells.[12,13,32]

To confirm sry$^+$ and sry$^+$/CK19$^+$ cells involving in liver regeneration, we first demonstrated that G-CSF mobilization increased CD34$^+$ HSCs in peripheral blood and liver graft, as was shown in PLTx + G-CSF rats from day 3 to 14 and in G-CSF + PLTx rats from day 1 to 7. Then the injury and regeneration of liver graft were evaluated, and we demonstrated that G-CSF mobilization after PLTx increased the survival rate of partial liver graft, improved liver injury that was recognized by damage scores; this was also confirmed by the decreased activities of serum hepatic enzymes AST and ALT. Liver regeneration could be assessed by different tissue-based indices such as liver weights, mitotic counts, DNA contents, and synthesis rates, and immunohistochemical staining of nuclear antigens.[33] These parameters clearly showed that the labeling mitotic indices and GRWR remained high on day 3 in PLTx + G-CSF group compared with G-CSF + PLTx and PLTx group. The data suggest that G-CSF administration after PLTx ameliorates the histological damage and promotes regeneration of partial liver graft.

In the G-CSF–mobilized groups, we found different effects of G-CSF administration before and after PLTx on liver regeneration. An interpretation of our results is that G-CSF could exert both direct and indirect effects on the liver through cytokine cascade and could potentially act as an unrecognized hepatocyte growth factor inducer. Indeed, it had been reported that hepatocyte growth factor levels in the serum of normal donors and G-CSF–mobilized patients increase almost sevenfold.[34] And G-CSF was also reported to enhance hepatocyte proliferation occurring after partial hepatectomy and fulminant hepatic failure (FHF). These data may explain why the capacity of liver regeneration in PLTx + G-CSF was higher than that in G-CSF + PLTx. Furthermore, priming mice and human beings with G-CSF had also been shown to promote migration of committed liver-specific stem cells preexisting in the bone marrow into circulation.[35] So another explanation of our findings is partly due to more CD34$^+$ HSCs migrating into liver graft and differentiating into hepatocytes and duct epithelial cells in the PLTx + G-CSF group. CD34$^+$ HSCs may affect liver regeneration in different ways. First, related to the time of G-CSF administration, more CD34$^+$ HSCs migrated into the liver graft in the PLTx + G-CSF than that in the G-CSF + PLTx group. Because the histology of the liver graft appeared a change in portal tract area and necrosis area, hence circulating marrow-derived CD34$^+$, HSCs might enter the liver in portal tract area and necrosis area, and differentiate into hepatocytes and duct epithelial cells. The origins of oval cells have been questioned. Although most researchers tend to believe that the cells reside in the canals of Hering, recent studies clearly indicate that at least a portion of the oval cell could be derived from bone marrow cells.[14,15,32] sry$^+$/CK19$^+$ cells, which appear the morphology of hepatic oval cells and cholangiocytes, exist in portal tract areas and suggest that HSCs might differentiate into hepatic oval cells, then into hepatocytes and duct epithelial cell. This could also be confirmed by sry$^+$ cells found around the portal tract area. On the other hand, circulating marrow-derived CD34$^+$ HSCs might enter the liver plates directly from the sinusoidal circulation. These cells were most often scattered throughout the parenchyma and could intercalate randomly into preexisting liver cords directly as hepatocytes, so we could find scattered sry$^+$ cells in liver lobule. Our results showed that bone marrow stem cells have the ability to repair liver injury, similar to what has been shown with ischemic injury to the myocardium.[23]

In our research, we reason that stem cells have the ability to repair liver injury, but we cannot precisely explain the actions of stem cells in liver regeneration, as was also concluded by Thorgeirsson and Grisham,[36] who thought that bone marrow stem cells do not contribute significantly to liver regeneration in most circumstances. Recently, several studies reported that bone marrow cells adopt the phenotype of other cell types by spontaneous cell fusion rather than by transdifferentiation.[11-13] In our study, it remains unknown whether sry$^+$ cells were generated by HSCs via transdifferentiation or fusion with existing parenchyma.

In our research, the survival after PLTx (female to male rats) was 50% lower compared with many of those previously described in the literature. One explanation for the low survival might be donor gender. Data from Brooks et al.[37] and Marino et al.[38] confirmed inferior graft and patient survival in males receiving the liver from a female donor. Furthermore, Gu et al.[28] recently assessed the influence of the male environment on the female liver graft by using a rat model. They found that male recipients of female livers had a less favorable outcome irrespective of graft size, and suggested that it was possibly related to an enhancement of ischemia-reperfusion injury by the lack of estrogen in male recipients of female grafts. Therefore, these clinical and experimental observations might support the phenomenon of low survival after female-to-male rat PLTx.

In conclusion, stem cell mobilization with G-CSF is appealing as a potential therapy for improving liver regeneration because it offers both ease of treatment and universality of application. The present results provide the conceptual basis for the development of therapeutic strategies aimed at stimulating the proliferation, mobilization, and targeting of these stem cells in an effort to enhance recovery from liver injury of PLTx.

REFERENCES

1. Kiuchi T, Kasahara M, Uryuhara K, Inomata Y, Uemoto S, Asonuma K, et al. Impact of graft size mismatching on graft prognosis in liver transplantation from living donors. Transplantation 1999;67:321-327.
2. Lo CM, Fan ST, Liu CL, Chan JK, Lam BK, Lau GK, et al. Minimum graft size for successful living donor liver transplantation. Transplantation 1999;68:1112-1116.
3. Ferrari G, Cusella-De Angelis G, Coletta M, Paolucci E, Stornaiuolo A, Cossu G, et al. Muscle regeneration by bone marrow–derived myogenic progenitors. Science 1998;279: 1528-1530.
4. Krause DS, Theise ND, Collector MI, Henegariu O, Hwang S, Gardner R, et al. Multi-organ, multi-lineage engraft-

ment by a single bone marrow–derived stem cell. Cell 2001;105:369-377.
5. Lin Y, Weisdorf DJ, Solovey A, Hebbel RP. Origins of circulating endothelial cells and endothelial outgrowth from blood. J Clin Invest 2000;105:71-77.
6. Asahara T, Murohara T, Sullivan A, Silver M, van der Zee R, Li T, et al. Isolation of putative progenitor endothelial cells for angiogenesis. Science 1997;275:964-967.
7. Brazelton TR, Rossi FM, Keshet GI, Blau HM. From marrow to brain: Expression of neuronal phenotypes in adult mice. Science 2000;290:1775-1779.
8. Mezey E, Chandross KJ, Harta G, Maki RA, McKercher SR. Turning blood into brain: Cells bearing neuronal antigens generated in vivo from bone marrow. Science 2000;290: 1779-1782.
9. Jang YY, Collector MI, Baylin SB, Diehl AM, Sharkis SJ. Hematopoietic stem cells convert into liver cells within days without fusion. Nat Cell Biol 2004;6:532-539.
10. Harris RG, Herzog EL, Bruscia EM, Grove JE, Van Arnam JS, Krause DS. Lack of a fusion requirement for development of bone marrow–derived epithelia. Science 2004; 305:90-93.
11. Ianus A, Holz GG, Theise ND, Hussain MA. In vivo derivation of glucose-competent pancreatic endocrine cells from bone marrow without evidence of cell fusion. J Clin Invest 2003;111:843-850.
12. Wang X, Willenbring H, Akkari Y, Torimaru Y, Foster M, Al-Dhalimy M, et al. Cell fusion is the principal source of bone marrow–derived hepatocytes. Nature 2003;422:897-901.
13. Vassilopoulos G, Wang PR, Russell DW. Transplanted bone marrow regenerates liver by cell fusion. Nature 2003; 422:901-904.
14. Petersen BE, Bowen WC, Patrene KD, Mars WM, Sullivan AK, Murase N, et al. Bone marrow as a potential source of hepatic oval cells. Science 1999;284:1168-1170.
15. Theise ND, Badve S, Saxena R, Henegariu O, Sell S, Crawford JM, et al. Derivation of hepatocytes from bone marrow cells of mice after radiation-induced myeloablation. Hepatology 2000;31:235-240.
16. Theise ND, Nimmakayalu M, Gardner R, Illei PB, Morgan G, Teperman L, et al. Liver from bone marrow in humans. Hepatology 2000;32:11-16.
17. Korbling M, Katz RL, Khanna A, Ruifrok AC, Rondon G, Albitar M, et al. Hepatocytes and epithelial cells of donor origin in recipients of peripheral-blood stem cells. N Engl J Med 2002;346:738-746.
18. Alison MR, Poulsom R, Jeffery R, Dhillon AP, Quaglia A, Jacob J, et al. Hepatocytes from non-hepatic adult stem cells. Nature 2000;406:257.
19. Wright DE, Bowman EP, Wagers AJ, Butcher EC, Weissman IL. Hematopoietic stem cells are uniquely selective in their migratory response to chemokines. J Exp Med 2002; 195:1145-1154.
20. Wright DE, Cheshier SH, Wagers AJ, Randall TD, Christensen JL, et al. Cyclophosphamide/granulocyte colony-stimulating factor causes selective mobilization of bone marrow hematopoietic stem cells into the blood after M-phase of the cell cycle. Blood 2001;97:2278-2285.
21. Lapidot T, Petit I. Current understanding of stem cell mobilization: The roles of chemokines, proteolytic enzymes, adhesion molecules, cytokines, and stromal cells. Exp Hematol 2002;30:973-981.
22. Orlic D, Kajstura J, Chimenti S, Limana F, Jakoniuk I, Quaini F, et al. Mobilized bone marrow cells repair the infracted heart, improving function and survival. Proc Natl Acad Sci U S A 2001;98:10344-10349.
23. Fukuhara S, Tomita S, Nakatani T, Ohtsu Y, Ishida M, Yutani C, et al. G-CSF promotes bone marrow cells to migrate into infarcted mice heart, and differentiate into cardiomyocytes. Cell Transplant 2004;13:741-748.
24. Theocharis SE, Papadimitriou LJ, Retsou ZP, Margeli AP, Ninos SS, Papadimitriou JD. Granulocyte-colony stimulating factor administration ameliorates liver regeneration in animal model of fulminant hepatic failure and encephalopathy. Dig Dis Sci 2003;48:1797-1803.
25. Theocharis SE, Margeli AP, Kittas CN. Effect of granulocyte colony-stimulating-factor administration on tissue regeneration due to thioacetamide-induced liver injury in rats. Dig Dis Sci 1999;44:1990-1996.
26. Omura T, Ascher NL, Emond JC. Fifty-percent partial liver transplantation in the rat. Transplantation 1996;62:292-293.
27. Kamada N, Calne RY. A surgical experience with five hundred and thirty liver transplantations in the rat. Surgery 1983;93:64-69.
28. Gu Y, Dirsch O, Dahmen U, Ji Y, He Q, Chi H, et al. Impact of donor gender on male rat recipients of small-for-size liver grafts. Liver Transpl 2005;11:669-678.
29. Kucia M, Ratajczak J, Reca R, Janowska-Wieczorek A, Ratajczak MZ. Tissue-specific muscle, neural and liver stem/progenitor cells reside in the bone marrow, respond to an SDF-1 gradient and are mobilized into peripheral blood during stress and tissue injury. Blood Cells Mol Dis 2004;32:52-57.
30. Kanazawa Y, Verma IM. Little evidence of bone marrow–derived hepatocytes in the replacement of injured liver. Proc Natl Acad Sci U S A 2003;100:11850-11853.
31. Wang X, Shundi G, McNamara Hao QL, Crooke G, Nolta J. Albuminexpressing hepatocyte-like cells develop in the livers of immune-deficient mice that received transplants of highly purified human hematopoietic stem cells. Blood 2003;101:4201-4208.
32. Lagasse E, Connors H, AI-Dhalimy M, Reitsma M, Dohse M, Osborne L, et al. Purified hematopoietic stem cells can differentiate into hepatocytes in vivo. Nat Med 2000;6: 1229-1234.
33. Assy N, Minuk GY. Liver regeneration: Methods for monitoring and their applications. J Hepatol 1997;26:945-952.
34. Fujii K, Ishimaru F, Kozuka T, Matsuo K, Nakase K, Kataoka I, et al. Elevation of serum hepatocyte growth factor during granulocyte colony-stimulating factor–induced peripheral blood stem cell mobilization. Br J Haematol 2004;124:190-194.
35. Kucia M, Ratajczak J, Reca R, Janowska-Wieczorek A, Ratajczak MZ. Tissue-specific muscle, neural and liver stem/progenitor cells reside in the bone marrow, respond to an SDF-1 gradient and are mobilized into peripheral blood during stress and tissue injury. Blood Cells Mol Dis 2004;32:52-57.
36. Thorgeirsson SS, Grisham JW. Hematopoietic cells as hepatocyte stem cells: A critical review of the evidence. Hepatology 2006;43:2-8.
37. Brooks BK, Levy MF, Jennings LW, Abbasoglu O, Vodapally M, Goldstein RM, et al. Influence of donor and recipient gender on the outcome of liver transplantation. Transplantation 1996;62:1784-1787.
38. Marino IR, Doyle HR, Aldrighetti L, Doria C, McMichael J, Gayawski T, et al. Effect of donor age and sex on the outcome of liver transplantation. Hepatology 1995;22: 1754-1762.